ARTICLES

High-resolution electron microscopy of discommensuration in the nearly commensurate phase on warming of $1T$-TaS$_2$

Takashi Ishiguro

Department of Electrical Engineering, Nagaoka University of Technology, Nagaoka, Niigata 940-21, Japan

Hiroshi Sato

School of Materials Engineering, Purdue University, West Lafayette, Indiana 47907-1289

In our previous paper [Phys. Rev. B **44**, 2046 (1991)], results of high-resolution transmission electron microscopy (HRTEM) at each stage of the complicated hysteretic phase transformation of $1T$-TaS$_2$ are described. Here, on warming from the commensurate (C) phase to the incommensurate (IC) phase, the triclinic (T) phase and the nearly commensurate (NC) phase on warming were found to serve as a discommensuration stage. Although both structures consist of similar discommensuration processes, the temperature dependence of the structure of the T phase can be explained quantitatively by a projected discommensuration model where domains with the commensurate structure are connected by the discommensurate network, but that of the NC phase on warming deviates from the prediction by the same model. In order to understand this discrepancy, a high-resolution (HR) observation of the NC phase on warming was extended to a temperature somewhat above the room temperature. The HR iamge obtained reveals, in the NC phase on warming, a "melting" of the commensurate domain into the discommensuration network. Based on this observation, a modified discommensuration model is proposed for the NC phase on warming as an intermediate phase in the commensurate-incommensurate phase transformation. In the Appendix, the difference in the image of the domainlike structure in the discommensurate stage obtained by TEM (projected image) and that of scanning tunneling microscopy (STM) [and of atomic force microscopy (AFM)] is pointed out. Then, the recently reported observation by STM and AFM of the discommensuration process in the NC phase on cooling is critically compared with our observation by TEM in the NC phase on warming.

I. INTRODUCTION

Earlier, electron microscopy of the incommensurate-commensurate phase transformation in $1T$-TaS$_2$, which has the CdI$_2$ type as the fundamental structure ($a_0 = 0.3363$ nm, $c_0 = 0.5896$ nm at room temperature[2]), was performed systematically (Ref. 1). It was found that, on cooling from the well-annealed incommensurate (IC) phase, the "nearly commensurate (NC) phase on cooling" appeared at ~ 347 K and transformed into the commensurate (C) phase at ~ 183 K. On the other hand, on warming from the C phase, the triclinic (T) phase appeared first at ~ 223 K, followed by the "NC phase on warming" at 280 K and the IC phase at ~ 354 K. The transition temperatures where the above phases appear in a cyclic thermal history agree well with the results obtained by specific-heat measurement.[3] The NC phase on cooling is essentially an incommensurate phase and no discommensuration process is observed by transmission electron microscopy (TEM). [After our observation published earlier[1] was completed, some important papers with respect to the phase transformation in $1T$-TaS$_2$ were published. Most of them concern the observation of a

discommensuration process in the NC phase on cooling by means of scanning tunneling microscopy[4−8,10−13] (STM) and/or atomic force microscopy[7,9] (AFM) and report the appearance of domainlike patterns similar to our observation in the warming stage.[1] Although the present interest is the elucidation of the discommensuration process in the warming stage, we discuss some important features of these works which are related to the present problem.] In contrast, in both the T phase and the NC phase on warming, a discommensurate network structure consisting of domains of the commensurate structure in the hexagonal lattice was observed by high-resolution (HR) electron microscopy.[1] The locations of the wave vectors which specify the modulated structures were obtained by electron diffraction. Then the phase transformation can be characterized as a trajectory in a map which specifies the change of the location of the modulation vector as shown in Fig. 1. We discuss, therefore, the phase transformation using this trajectory as a reference.

An idealized model in which domains of hexagonal shape of the same size are assumed for the discommensurate network, based on the observed HR images, was proposed in Ref. 1 as shown in Fig. 2 and the observed tra

jectory of the T phase with temperature was explained by this model (Fig. 1). In other words, the change of the diffraction pattern of the T phase with temperature can be understood as the decrease in size of the domains having commensurate structure and, hence, as the increase in the relative area of discommensurate networks (the original hexagonal lattice) with temperature. However, the trajectory of the NC phase on warming was found to deviate gradually with temperature from the trajectory expected from the model.

The present paper tries to elucidate this deviation in the NC phase on warming. HR images of the NC phase on warming are taken in a temperature region where the deviation from the idealized model becomes more appreciable. By examining the HR images thus taken, a modification for the discommensurate structure is proposed to understand the behavior of the NC phase on warming.
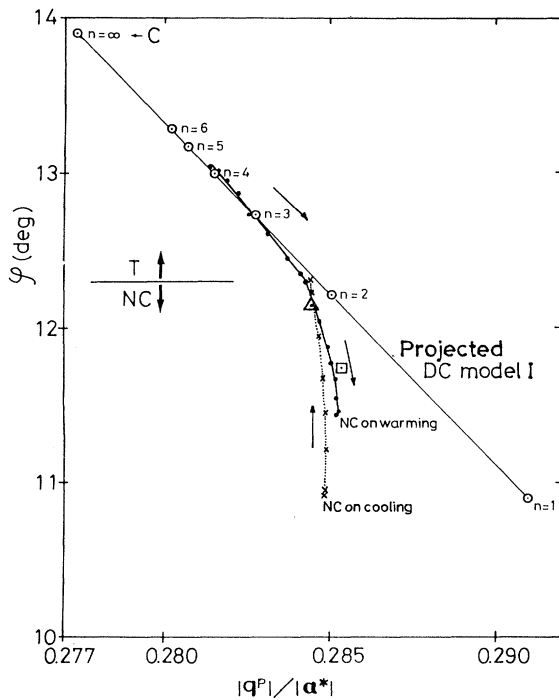

FIG. 2. Schematic representation of the C phase and an idealized model for projected discommensuration network (the PDC model I). (a) The C phase. The circle indicates the location of the star-shaped cluster and the number indicates the location of the center of the star-shaped cluster for indicating possible stacking positions. The rhombus indicates the unit cell of the C phase. (b) and (c): Arrangement of hexagonal commensurate domains of the size $n = 1$ and 2 (the length of the side of the hexagon of the commensurate domain is the unit for the size of the rhombus of the unit cell of the C phase) arranged with relative shifts with the shift vectors 8, 7, and 11 (this is equivalent to the shifts of 5, 6, and 2).

FIG. 1. Trajectory in the $|q^{P}|/|a^{*}|$ vs ϕ diagram for the phase transformation of $1T$-TaS_2 from the C phase to the NC phase on warming through the T phase. Solid circles indicate the observed change on warming. The arrows along the trajectories are directions of change with temperature. The thin line indicates the relation $|q^{P}|/|a^{*}| - \phi$ calculated from the idealized PDC model I shown in Fig. 2 for the discommensurate network (Ref. 1). An empty triangle indicates the location corresponding to the high-resolution (HR) image taken at 301 K in Ref. 1. An empty square indicates the location for the present HR observation at 333 K. The deviation of the observed trajectory from the trajectory of the PDC model I is the focus of the study. The trajectory for the NC phase on cooling is added for reference.
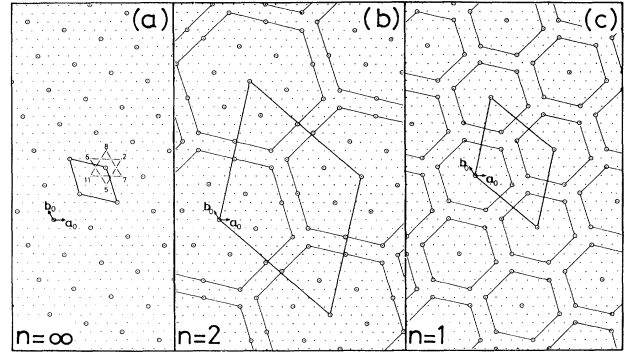
II. EXPERIMENT

Single crystals of $1T$-TaS_2 were grown by means of a vapor transport technique at the Central Material Preparation Facility of Purdue University. As pointed out in the previous paper (Ref. 1), the phase transformations of $1T$-TaS_2 are strongly hysteretic. Therefore, to observe the NC phase on warming in a consistent fashion, the specimen should go through the same thermal history each time and thus through the C phase at low temperatures.[1] The specimen was cleaved along the basal plane of the crystal and was fixed on a copper mesh by silver epoxy glue (EPO-TEK H20E). The specimen was first kept at 375 K (in the IC phase) on a hot plate for more than 1 h, and then the annealed specimen was encapsulated (in the NC phase on cooling) and cooled down to liquid-nitrogen temperature (in the C phase) for 30 min. After keeping it for about 1 h at liquid-nitrogen temperature, the specimen in the C phase was then slowly warmed up to room temperature (reaching the NC phase on warming via the T phase), and was set on the double-tilt liquid-helium specimen holder (Gatan, Ltd.).

For the high-resolution TEM observation, a JEOL 2000FX electron microscope with a point-to-point resolution of 0.29 nm at Purdue University was used. To carry out the HR observation at temperatures above room temperature, a stable condition for the specimen must be achieved. The following method was used for this purpose. The coolant tank of the specimen holder was filled with distilled water and warmed up by a heater immersed in it. Then the specimen temperature was controlled by
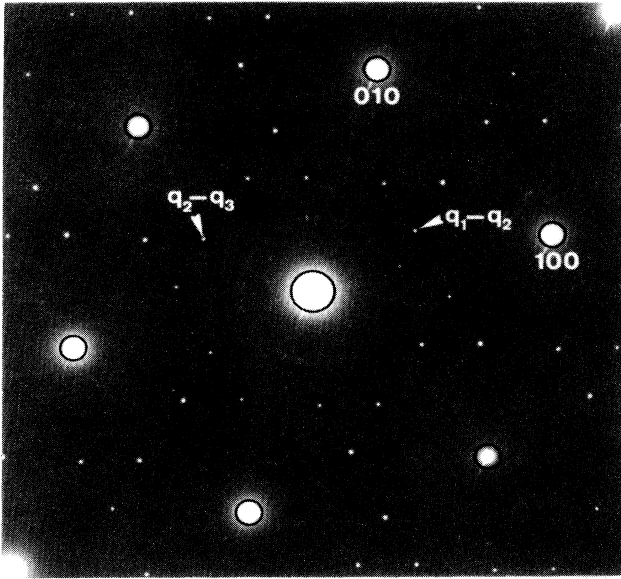
FIG. 3. [001] diffraction pattern of the NC phase on warming at 333 K. The differences $q_1 - q_2$, etc., correspond to the secondary reflections. Circles represent the bandpass filter used for the image processing.

both the heater in the coolant tank and the specimen heater which is originally included in the holder. At 333 K, HR images of the NC phase on warming were thus taken using the minimum dose system under a quite stable condition.

The HR images obtained were image processed in the following way because they contained noise. The information of an enlarged raw image was digitized by the image scanner GT-2000 (Seiko Epson Co.) with a spatial resolution of 120 dpi and a gradation of 8 bits per pixel. The digital information with a 256×256 matrix was Fourier transformed by the fast Fourier transform (FFT) method. In reciprocal space, the data of the image were taken using a proper Fourier bandpass filter shown in Fig. 3 by black circles and then inversely Fourier transformed back into real space. The calculated, processed images were recorded by the film recorder FR-1000 (Japan Avionics Co.).

III. RESULTS AND DISCUSSION

To clarify the physical situation involved in the phase transformation of $1T$-TaS_2 on warming from the C phase, the description with respect to the projection of the fundamental modulation wave vectors q_1, q_2, and q_3 on the basal plane is explained first.[1] The q vectors do not lie on the basal plane which is determined by the fundamental reciprocal lattice vectors of a^* and b^* for the fundamental structure of $1T$-TaS_2. However, the secondary reflections such as $q_1 - q_2$, etc. appear on the basal plane (Fig. 3). Therefore the projections of the fundamental modulation wave vectors on the basal plane, q_1^P, q_2^P, and

q_3^P can be determined from the locations of the secondary reflections. The angle ϕ indicates the deviation of q_1^P from the b^* axis.

Figure 1 shows the phase transformation on warming from the C phase as a trajectory in the coordinate system of ϕ vs $|q^P|/|a^*|$. This information is obtained from observations of the ϕ temperature and $|q^P|/|a^*|$-temperature relations.[1] Small filled circles connected by a thick line indicate the observed points. Here, the line above $\phi = 12.3°$ corresponds to the T phase, and the line with angle less than $12.3°$ corresponds to the NC phase on warming. The open circles connected by a thin line in this figure indicate the trajectory expected from the idealized model of a discommensurate network, which was already proposed as shown in Fig. 2 in the previous paper.[1] Hereafter, we call this idealized model the projected discommensuration (DC) model (see the Appendix) I (PDC model I). In the figure, the behavior of the NC phase on cooling is added as a dotted line with data points for reference. The vertical dotted line here indicates the pure rotation of the NC phase on cooling with lowering temperature.

Figure 2(a) shows the $\sqrt{13} \times \sqrt{13}$ structure of the C phase.[14] The vectors a_0 and b_0 correspond to the fundamental translation vectors in the c plane. Each open circle corresponds to the location of a star-shaped cluster which contains 13 Ta atoms per one single layer. The numbers $2, 5, 6, \ldots$, etc., indicate the locations of the center of the star-shaped cluster for possible stacking positions in the C phase.[1] Figures 2(b) and 2(c) show examples, $n = 1$ and $n = 2$, of the PDC model I.[1] In this model, the system consists of hexagonal commensurate domains and a discommensurate network. The number n indicates the length of the side of the hexagon of the commensurate domain which is characterized by the size of the rhombus of the unit cell of the commensurate structure as shown in Fig. 2(a). The commensurate domains are arranged with relative shifts with the shift vectors 8, 7, and 11 which are equivalent to shifts of 5, 6, and 2. The calculated trajectory from the PDC model I has been shown in Fig. 1 with a thin line. It is clear that the observed trajectory of the T phase changes along the thin line from $n = 4$ to near $n = 2$ represented by the idealized PDC model I. The projected discommensurate structure as revealed by a HR image in the NC phase on warming is essentially the same as that in the T phase,[1] although the stacking order changes at the transition from T to NC.[1] However, the trajectory of the NC phase on warming gradually deviates from the line of the model. We deal with this deviation in this paper.

The location of the HR image on the trajectory of the NC phase on warming that we had observed in Ref. 1 is indicated by a triangle in Fig. 1. The image obtained was close to that of the PDC model I with $n = 2$.[1] The deviation of the location of the triangle from the trajectory of the PDC model I is relatively small. Therefore, it is natural that the character of the NC phase on warming (Fig. 22 of Ref. 1) just after transformation from the T phase deviates little from that of the T phase. To understand the deviation in the NC phase from that of the PDC model I, it is therefore necessary to observe HR images of

the typical NC phase above room temperature. The location of the HR image taken at this time is shown in Fig. 1 as a square. The observed temperature is 333 K and the location is calculated from the [001] diffraction pattern as shown in Fig. 3. Here, it is expected that the corresponding HR image contains a typical structural feature of the NC phase on warming.

The printed raw [001] HR image has been processed using a bandpass filter indicated by circles in Fig. 3. In the processed image of Fig. 4, a point-to-point resolution of 0.29 nm is achieved. This whole square area of Fig. 4 corresponds to the area of Fourier transformation with a matrix of 256×256. A group of discontinuous lines that connects the high-intensity white dots with the period of the commensurate structure in the c plane can be detected. A characteristic contrast observed here is that a low-intensity spot is surrounded by three nearest-neighboring high-intensity spots as indicated by a circle in Fig. 4. Its enlargement is shown at the corner of this figure. This type of group of spots having this contrast is selected from the image and is schematically mapped as shown in Fig. 5 using an empty circle and three dots. The rhombus with thick lines connecting open circles corresponds to the unit cell of the C phase in the c plane as shown in Fig. 2(a). It can be seen as an assembly of local hexagonal networks with the period of the commensurate phase. The translational vectors connecting these commensurate domains to each other are classified into two groups according to their shift vector lengths. The first group has relatively short shift vectors such as 8, 7, and 11 (and/or 5, 6, and 2) as shown in Fig. 2(a). These vectors are the same as the vectors defined in the projected discommensurate network in the PDC model I [Figs. 2(b)
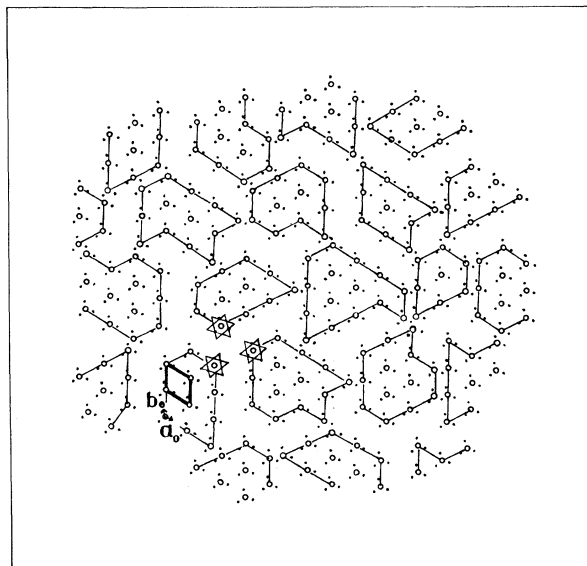
FIG. 5. Projected domain structure of the NC phase on warming at 333 K. This is created from the image of Fig. 4 by taking locations having the characteristic local image contrast shown in the circle (and shown magnified in the inset) in Fig. 4. A star shape with an empty circle as a center represents the star-shaped cluster of Fig. 2(a). The rhombus with thick lines corresponds to the unit cell of the C phase [Fig. 2(a)]. The vectors connecting the nearest-neighbor commensurate domains are classified into two groups, i.e., the relatively shorter vectors from 0 to 8, 6, and 11, respectively (equivalent to 5, 6, and 2) as shown in Fig. 2(a) and the relatively longer vectors of $2(8+\mathbf{b}_0)$, $2(2+\mathbf{a}_0+\mathbf{b}_0)$, and $2(7+\mathbf{a}_0)$ [equivalent to $2(5-\mathbf{b}_0)$, $2(11-\mathbf{a}_0-\mathbf{b}_0)$, and $2(6-\mathbf{a}_0)$].
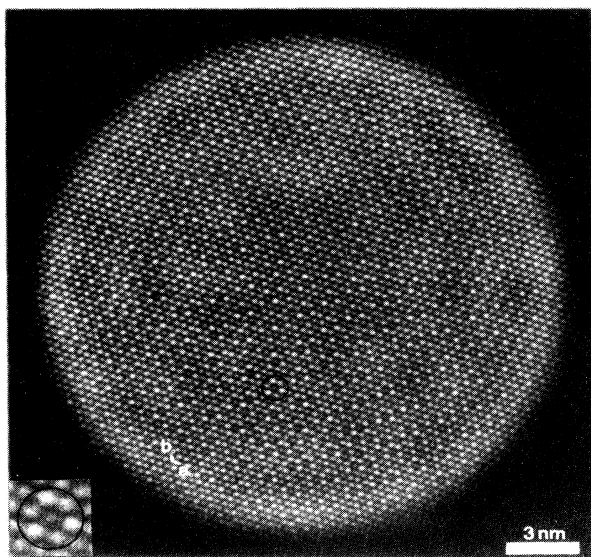

FIG. 4. Processed [001] high-resolution image corresponding to the diffraction pattern of Fig. 3. The image contrast enclosed by a circle indicates a characteristic local image contrast in this image. Its enlargement is shown at a corner.

and 2(c)]. The second group has relatively long shift vectors of $2(8+\mathbf{b}_0)$, $2(2+\mathbf{a}_0+\mathbf{b}_0)$, and $2(7+\mathbf{a}_0)$ [and/or $2(5-\mathbf{b}_0)$, $2(11-\mathbf{a}_0-\mathbf{b}_0)$, and $2(6-\mathbf{a}_0)$]. The difference in length between the second and the first group is just an edge of the unit cell of the $\sqrt{13}\times\sqrt{13}$ structure [Fig. 2(a)].

Based on the above observation, an idealized projected discommensurate network model is proposed as shown, for example, in Figs. 6(a) and 6(b). Hereafter, we refer to this model as the projected DC model II (PDC model II). In this model, the shape of the commensurate domain is assumed to be a hexagon like the one used in the PDC model I. Here, n also characterizes the length of the side of the hexagon of the commensurate domain as in the PDC model I. With respect to the projected discommensurate network region, vectors of the second group obtained from Fig. 5 are used for the relation between the nearest-neighbor hexagons. From the PDC model II, the relation between n and ϕ and $|\mathbf{q}^P|/|\mathbf{a}^*|$ can be calculated as

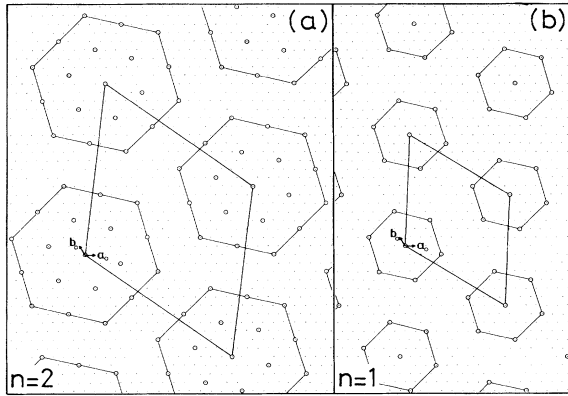$$\phi_n = \tan^{-1}\{(3n+2)^2/[\sqrt{3}(2\ln^2+34n+16)]\} \qquad (1)$$

and

FIG. 6. An idealized projected discommensuration network called the PDC model II. For the distance between nearest-neighbor hexagons, the longer shift vectors found from Fig. 5 are used. The number n represents the size of the commensurate domain in the same way as that of the PDC model I [Figs. 2(b) and 2(c)]. The rhombuses in (a) and (b) represent the unit cell of each example of the model II for $n = 2$ and 1, respectively.
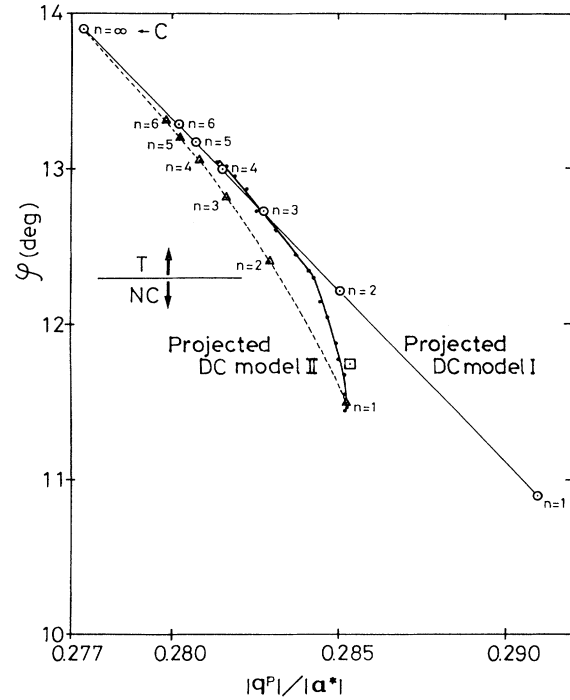

FIG. 7. Comparison between the observed trajectory with the calculated trajectories from the PDC models I and II. The dashed line indicates the trajectory of the PDC model II. The other part is the same as Fig. 1. The observed trajectory of the NC phase on warming separates from the line of the PDC model I at the T-NC transition point and coincides with the position of $n = 1$ of the PDC model II.

$$|q_n^P|/|a^*| = 3(n+1)/\{\sqrt{3}(5n+2)\sin\phi_n$$

$$+ (9n+10)\cos\phi_n\} . \qquad (2)$$

In Fig. 7, $\phi_n - |q_n^P|/|a^*|$ thus represents a curved line shown as the dashed line and $n = \infty$ corresponds to the C phase as in the PDC model I.

It is clear that the observed trajectory of the NC phase on warming exists between the trajectories of the PCD models I and II. With temperature, the observed trajectory separates from that of the PDC model I and gradually approaches the point $n = 1$ of the PDC model II. After this, the NC phase on warming transforms into the IC phase. This observation indicates that the domain size of $n = 1$ is the minimum size for the commensurate domains to be stable. The HR image of Fig. 4 whose state in $\phi - |q^P|/|a^*|$ is indicated by a square in Fig. 7 shows an intermediate feature between the two idealized PDC models. As for the width of the projected discommensurate network, vectors connecting commensurate domains can be classified into two groups and they coexist. In other words, they are either wider as in the PDC model II or narrower as in the PDC model I. The area of each commensurate domain can be estimated by counting the number of isolated circles in each domain in Fig. 5. The average number of circles in one domain is about 11 ± 2. (This value is between 19 for the hexagon with $n = 2$ and 7 for the hexagon with $n = 1$.) From this result, it is concluded that the change with temperature in the NC phase on warming is a process where commensurate domains with the size of about $n = 2$ melt into the discommensurate region until the size of them becomes $n = 1$.

In the commensurate-incommensurate phase transformation, McMillan proposed a concept of discommensuration[15] which is essentially a compromise form in real

space between the commensurate period and the incommensurate period. In the T phase obtained from the C phase on warming, discommensurations are introduced to form commensurate domains separated by the discommensurate network. With change in temperature, these domains become smaller with an increasing density of discommensurate network. Eventually, both an increase in the width of the discommensuration network and a melting of the commensurate domain occur simultaneously. Apparently, this change corresponds to the NC phase on warming, in addition to the stacking behavior explained in Ref. 1. Thus the present study has clarified the difference in behavior of discommensuration between the T phase and the NC phase on warming in addition to the stacking behavior explained in Ref. 1.

ACKNOWLEDGMENTS

APPENDIX: DISCOMMENSURATION STRUCTURE IN THE NC PHASE ON COOLING

Some important papers with respect to the phase transitions of $1T$-TaS_2 have recently been published. Most of these contributions concern the observation of a discommensurate structure in the NC phase on cooling by means of scanning tunneling microscopy[10–13] and atomic force microscopy.[7,9] On the other hand, our observation by means of HRTEM could not detect the existence of such a discommensurate structure in the NC phase on cooling.[1] Therefore, the success in the observation of the discommensuration process in the NC phase on cooling by STM is extremely important to understand the mechanism of the phase transition involved. In addition, because the observations by means of STM and AFM are complementary to those by means of TEM, a comparison of the results of these two different methods is expected to be instructive in elucidating the mechanism, although our interest here is to understand the discommensuration process in the NC phase on warming. Here, we use the term the "*projected* discommensuration model" for the DC model used in the previous paper based on the difference between the observed images of TEM and those of STM (or AFM) for this comparison.

First, our attention is directed toward conflicting reports with respect to the discommensurate structure in the NC phase on cooling based on the observations by means of STM and AFM. Wu and Lieber concluded that there were commensurate domains separated by diffuse domain walls[4–6] while Slough et al.[7,8] and Garnaes et al.[9] conclude that the NC phase had a domainlike structure due to a continuous incommensurate charge-density wave with a strong continuous amplitude modulation. Both conclusions on the domain structure are qualitatively the same, but the essential difference lies in whether the domain is commensurate[4–6] or incommensurate.[7–9]

Based on our TEM observation,[1] we concluded that the NC phase on cooling was intrinsically incommensurate and the NC phase on warming had commensurate domains separated by a background hexagonal structure as a discommensurate network. In order to understand such a discrepancy as well as the different results obtained for the NC phase on cooling as mentioned above, it is necessary to compare the two following situations. The first is that, as we emphasized in our previous paper,[1] to obtain a consistent result in the phase transformation of $1T$-TaS_2, a careful treatment of the thermal history of the specimen is necessary. The second is that the difference in observation method, i.e., TEM and STM and/or AFM, should be considered. In the first place, the appearance of a discommensurate structure consisting of commensurate domains is generally an indication that the specimen is heated from the commensurate structure.[16] Indeed, the domainlike structure reported by Wu and Lieber[5] is very closely related to that observed by us[1] in the NC phase on warming. In addition, the temperature dependence of both the direction of the modulation wave and the size of the commensurate domains reported is consistent with our results in the warming stage rather

than the cooling stage. In other words, the thermal history of their specimens does not seem to be consistent with that of our experiment. With respect to the second point, in the case of TEM observation, where the images correspond to the projected potential, one has to note that the observation is not sensitive to a shift along the projected direction but rather sensitive to the horizontal shift. In contrast, the STM and/or AFM observation is sensitive to the vertical shift on the surface. Based on the above considerations, if a discommensurate structure with commensurate domains like that mentioned by Wu and Lieber exists in the NC phase on cooling, commensuration domains as shown in Fig. 4 might have been observed in our TEM image of the NC phase on cooling because they have the same nature as those observed in the NC phase on warming. However, if the structure of the NC phase on cooling is the structure developed from the incommensurate phase as mentioned by Slough et al.[7,8] and Garnaes et al.[9] it is possible that we did not recognize the domain structure in the TEM image. If all these conditions are considered, it seems probable that the specimens used by Wu and Lieber[5] had experienced the C phase in their thermal history.

Now, there is still a discrepancy between our observation and the result of Wu and Lieber[5] with respect to the domain-domain phase shift. They reported that it has a lattice period of a_0 and the same phase shift was also observed by STM in the T phase by Thomson et al.[17] However, it should be noted that the HRTEM image is a superposition of layers having different stacking positions from one another. In our previous paper,[1] the relative
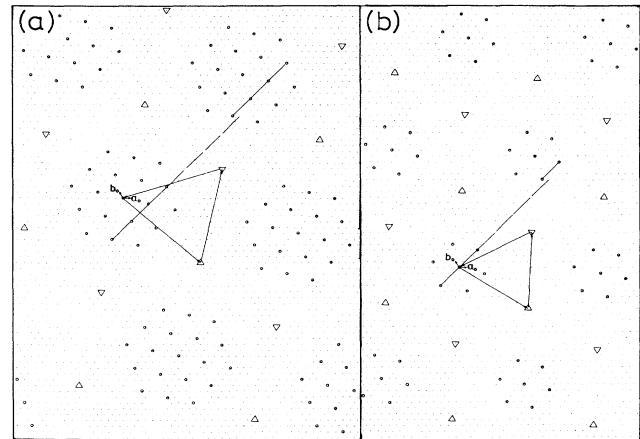

FIG. 8. Commensurate domain model for one layer. (a) and (b) are deduced from the PDC model I with $n = 2$ and the projected DC model II with $n = 1$, respectively. The hexagonal arrangement of circles makes one commensurate domain. The relative phase shift between nearest-neighbor hexagonal commensurate domains is a_0. $\triangle$ indicates the centers of the hexagonal commensurate domains of the second layer. ∇ indicates those of the third layer. Arrows connecting the center of the hexagonal commensurate domain of the first layer, the center $\triangle$ of the second layer, and the center ∇ of the third layer with each other indicate the stacking relation along the projected direction.

separation of the independent primary reflections (q_1, q_2, and q_3) from the a^*-b^* plane along the c^* direction with respect to the unit reciprocal layer distance (ζ in $|c^*|$ units) was measured. ζ in the T phase deviates somewhat from $\frac{1}{3}$ and ζ of the NC phase on warming is $\frac{1}{3}$ within the experimental error.[1] This means that the stacking of the modulated layer has a period of $3c_0$ in the region of the T phase and of the NC phase on warming.

To obtain a consistent result concerning both the stacking period of the layers and the phase shift, the projected DC models I and II are adopted as a superposition of the distributions on the three layers with different projected stacking positions on the a-b plane. Figure 8(a) schematically shows the one-layer structure which is deduced from the PDC model I with $n = 2$. A hexagonal arrangement of circles with a commensurate period makes a commensurate domain. The structure of one layer is composed of these hexagonal commensurate domains with $n = 2$ and a quite wide domain wall, i.e., discommensurate region. Such a wide discommensurate region, however, is comparable to the theoretical prediction by Nakanishi and Shiba.[18] The center of the hexagonal commensurate domain is distributed to make a hexagonal lattice. The phase shift across a domain wall in this model is one atomic period of a_0 as shown by referring to the extrapolated lines connecting circles with a commens-

urate period in Fig. 8.[4–6] The locations of the commensurate domain centers for the second and the third layers are marked by triangles and inverse triangles, respectively. The superposition of these three layers coincides with the PDC model I with $n = 2$. A similar procedure for the PDC model II with $n = 1$ gives the one-layer structure shown in Fig. 8(b). Therefore, it can be interpreted that the change in one layer of the NC phase on warming is the change from Fig. 8(a) to Fig. 8(b). It is thus apparent that the results of our observation and the result of Wu and Lieber are consistent with respect to the phase shift. This is the reason why we call our model the "projected" DC model.

The difference in the structural features between the T phase and the NC phase on warming with respect to the deviation of the stacking period from $3c_0$ can possibly be deduced from the above model. Because of the melting of the commensurate domains, in the NC phase on warming, each commensurate domain for one layer is stacked above the discommensurate region of the lower layer, as shown in Fig. 8(b). On the other hand, the PDC model I for the T phase ($n \geq 2$) suggests a partial overlapping at the edge of the commensurate domains between nearest-neighboring layers. Such an overlapping increases the energy of the Coulomb interaction[17] between the layers and may cause the deviation of stacking from $\zeta = \frac{1}{3}$.

[1]T. Ishiguro and H. Sato, Phys. Rev. B **44**, 2046 (1991).

[2]F. L. Givens and G. E. Fredericks, J. Phys. Chem. Solids **38**, 1363 (1977).

[3]S. C. Bayliss, A. M. Ghorayeb, and D. R. P. Guy, J. Phys. C **17**, L533 (1984).

[4]X. L. Wu and C. M. Lieber, Science **243**, 1703 (1989).

[5]X. L.Wu and C. M. Lieber, Phys. Rev. Lett. **64**, 1150 (1990).

[6]X. L. Wu and C. M. Lieber, J. Vac. Sci. Technol. B **9**, 1044 (1991).

[7]C. G. Slough, W. W. McNairy, R. V. Coleman, J. Garnaes, C. B. Prater, and P. K. Hansma, Phys. Rev. B **42**, 9255 (1990).

[8]C. G. Slough, W. W. McNairy, C. Wang, and R. V. Coleman, J. Vac. Sci. Technol. B **9**, 1036 (1991).

[9]J. Garnaes, S. A. C. Gould, P. K. Hansma, and R. V. Coleman, J. Vac. Sci. Technol. B **9**, 1032 (1991).

[10]B. Burk, R. E. Thomson, A. Zettl, and J. Clarke, Phys. Rev. Lett. **66**, 3040 (1991).

[11]R. V. Coleman, W. W. McNairy, and C. G. Slough, Phys. Rev. B **45**, 1428 (1992).

[12]M. Remskar, A. Prodan, and V. Marinkovic, Surf. Sci. **287**, 409 (1993).

[13]W. Han, R. A. Pappas, E. R. Hunt, and R. F. Frindt, Phys. Rev. B **48**, 8466 (1993).

[14]R. Brouwer and F. Jellinek, Physica B **99**, 51 (1980).

[15]W. L. McMillan, Phys. Rev. B **14**, 1496 (1976).

[16]Y. Koyama, Z. P. Zhang, and H. Sato, Phys. Rev. B **36**, 3701 (1987).

[17]R. E. Thomson, U. Walter, E. Ganz, J. Clarke, A. Zettl, P. Rauch, and F. J. Disalvo, Phys. Rev. B **38**, 10 734 (1988).

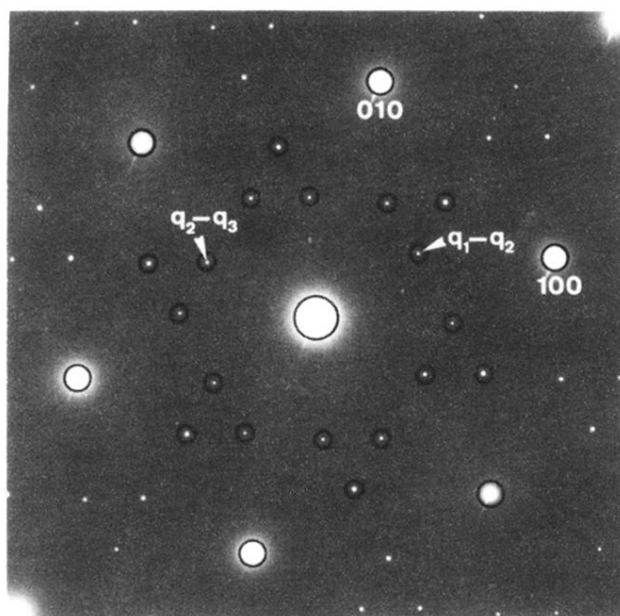[18]K. Nakanishi and H. Shiba, J. Phys. Soc. Jpn. **43**, 1839 (1977).

FIG. 3. [001] diffraction pattern of the NC phase on warming at 333 K. The differences $\mathbf{q}_1 - \mathbf{q}_2$, etc., correspond to the secondary reflections. Circles represent the bandpass filter used for the image processing.
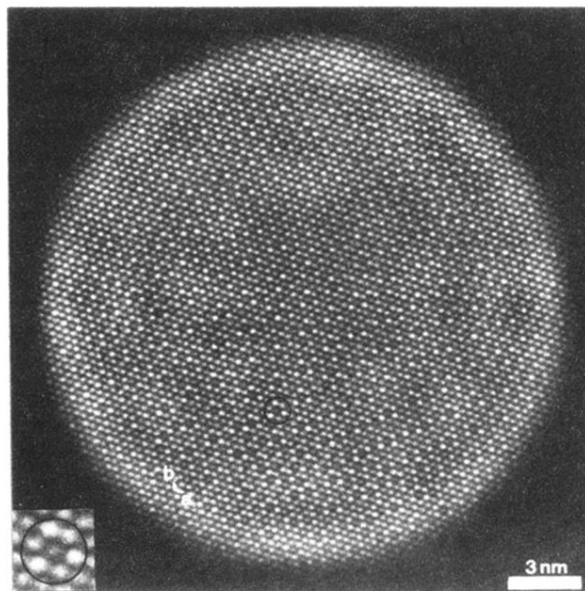
FIG. 4. Processed [001] high-resolution image corresponding to the diffraction pattern of Fig. 3. The image contrast enclosed by a circle indicates a characteristic local image contrast in this image. Its enlargement is shown at a corner.